Transient surface photovoltage spectroscopy of diamond

Cite as: AIP Advances 12, 065206 (2022); doi: 10.1063/5.0089398
Submitted: 8 March 2022 • Accepted: 23 May 2022 •
Published Online: 7 June 2022

Th. Dittrich[a)]

AFFILIATIONS

Helmholtz Zentrum Berlin für Materialien und Energie GmbH, Institut für Si-Photovoltaik, Schwarzschildstr. 8, D-12489 Berlin, Germany

[a)]Author to whom correspondence should be addressed: dittrich@helmholtz-berlin.de

ABSTRACT

Contactless and highly sensitive probing of electronic transitions in diamond over a wide spectral range from near infrared to deep ultraviolet is still challenging. Surface photovoltage (SPV) signals depend on electronic transitions and transport phenomena leading to charge separation in space and allow for a contactless study of electronic transitions. Here, transient SPV spectroscopy in an arrangement with a charge amplifier and a laser tunable over a wide range was applied to study an undoped diamond single crystal between 0.8 and 5.9 eV at room temperature in ambient air. SPV transients were measured without and with weak visible bias light, which allowed for suppression of possible parasitic contributions in SPV signals not related to diamond and distinction of processes of charge separation that were independent of band bending. Transitions at 1.0 and 3.1 eV led to preferential separation of photogenerated holes toward the surface. In contrast, a transition at 1.8 eV caused preferential separation of photogenerated electrons toward the surface. Transitions near the indirect bandgap of diamond were observed at 5.27, 5.32, 5.48, and 5.53 eV and could be assigned to absorption assisted (i) by an indirect exciton and absorption of longitudinal optical and acoustic phonons, (ii) by absorption of transverse acoustic phonons, (iii) by emission of transverse acoustic phonons, and (iv) by emission of longitudinal optical and acoustic phonons, respectively. Charge separation under excitation at 5.27 eV was caused by directed charge transfer at/near the diamond surface after exciton diffusion followed by exciton dissociation.

I. INTRODUCTION

Diamond has a large indirect bandgap of 5.47 eV,[1] making it, in combination with high electron and hole mobilities (close to 1000[2] and 2000[3] cm^2/V^{-1} s at room temperature in n- and p-type doped diamond, respectively), high breakdown field strengths (13–20 MV/cm[4,5]), and extremely high thermal conductivity (20 W cm^{-1} K^{-1}[6]), unique for high-temperature and high power electronic applications. Furthermore, specific properties of defects in diamond, such as nitrogen-vacancy centers, opened up, for example, applications for controlling in-plane Schottky junctions,[7] new read-out protocols for spin states,[8] or high-performance detection of vacuum ultraviolet, extreme ultraviolet, and x rays.[9] In addition, high environmental robustness, possibility of surface functionalization,[10] and surface transfer doping[11] make diamond highly attractive for photocatalytic and specific electronic and sensor applications.

For further development, the contactless characterization of electronic defect states and electronic transitions in bulk diamond and at diamond surfaces is of great interest. Aside from the identification of transition energies, for further development of optoelectronic devices based on diamonds, it is essential to also understand the direction and mechanisms of charge separation and relaxation. Surface photovoltage (SPV) signals are caused by the separation of photogenerated charge carriers in space. SPV signals can be applied for highly sensitive studies of electronic properties of photoactive materials without the need for contact preparation.[12,13] Excitation of sub-bandgap states in diamond generated SPV signals, as shown by Kelvin force microscopy,[14] secondary electron emission,[15] or measurements of contact potential differences.[16] Furthermore, it was shown by photoelectron emission that SPV signals can sustain temperatures up to 700 K on hydrogenated diamond.[17] An onset of SPV signals at excitation above the indirect bandgap of diamond was recently shown by UV-AC-SPV.[18] Despite the existence of SPV

being demonstrated for diamond in several works, the extraction of transition energies by SPV still remains challenging for diamond.

In semiconductors with a wide bandgap, the relaxation time of photogenerated charge separated in space can be relatively long with respect, for example, to the dielectric relaxation time.[13,19] Therefore, the overall distribution of charge carriers, and consequently SPV signals, can sensitively depend on the measurement conditions. Transient SPV spectroscopy[13,20–22] is sensitive to the transition dependent relaxation of photogenerated charge carriers separated in space. This work is aimed to qualitatively show that transitions below and around the bandgap of diamond can be well distinguished and studied by transient SPV spectroscopy whereas a charge amplifier[22] was used for the detection of SPV signals. Furthermore, sub-bandgap bias light was used to discriminate parasitic transient phenomena and transient phenomena, which were independent of the built-in electric field in order to unambiguously identify electronic transitions in undoped diamond by transient SPV spectroscopy. The identified electronic transitions were related to defect states and to absorption assisted by indirect excitons and phonons. It was found that dissociation of excitons can play an important role in the evolution of transient SPV signals in diamond.

II. EXPERIMENTAL

An undoped CVD diamond crystal (orientation [100], size $10 \times 10 \times 0.5$ mm^3, Diamond Foundry) was investigated by transient SPV spectroscopy in ambient air at room temperature. The diamond surface was not treated before measurements. The sample holder was made of stainless steel. Transient SPV spectroscopy measurements were performed with a fixed perforated electrode, a charge amplifier (resolution time 7 ns), an oscilloscope card (Gage, CSE 1622-4GS), a tunable Nd:YAG laser for excitation (duration time of laser pulses 3–5 ns, range of wavelengths 216–2600 nm, EKSPLA, NT230–50, equipped with a spectral cleaning unit), and a tunable beam expander. The SPV signal height was calibrated with a periodic square wave signal (1 V_{pp}) applied at the back side of the sample. The repetition rate of the laser pulses was 0.5 Hz, and 10 transients were averaged. For more details see also Refs. 20 and 22. A warm white light-emitting diode (LED) (about 100 μW/cm^2 at the electrode) was used for measurement under bias light illumination.

III. RESULTS AND DISCUSSIONS

Figure 1 shows the contour plots of transient SPV spectroscopy, i.e., the color-coded SPV signals as a map in photon energy and time, for diamond measured (a) without and (b) with bias light from the white LED. The markers t1–t6 give points in characteristic regions. As a remark, SPV signals of diamond did not level out within the range shown (99 ms). For measurements without and with bias light, positive SPV signals of up to several mV were set at photon energies above 1 and 1.5 eV (region with t1). The sign of the SPV signals changed from positive to negative at photon energies between 2.2 and 2.3 eV. The negative SPV signals were several mV between 2.3 and about 3.5 eV (region with t2), about 10–15 mV between 3.6 and about 5 eV (region with t3), several mV between about 5 and 5.3 eV (region with t4), tens of mV between 5.3 and 5.6 eV (region with t5), and more than 100 mV above 5.5 eV for the measurement with bias light (region with t6). This means that the SPV signals measured at excitation above the bandgap of diamond increased under bias light.

SPV signals measured on the diamond might be influenced by parasitic SPV signals arising due to illumination of the sample holder and/or other components and materials used such as the electrode and wires. In order to get an impression about a suitable influence of the sample holder on SPV measurements of diamond, Fig. 1(c) shows the contour plot of the bare sample holder. Positive SPV signals of up to several mV were present for excitation at photon energies of above about 3 eV whereas the regions between 3 and 4 eV and between 4.9 and 5.7 eV were significant for times up to several μs or longer than 100 ms, respectively.

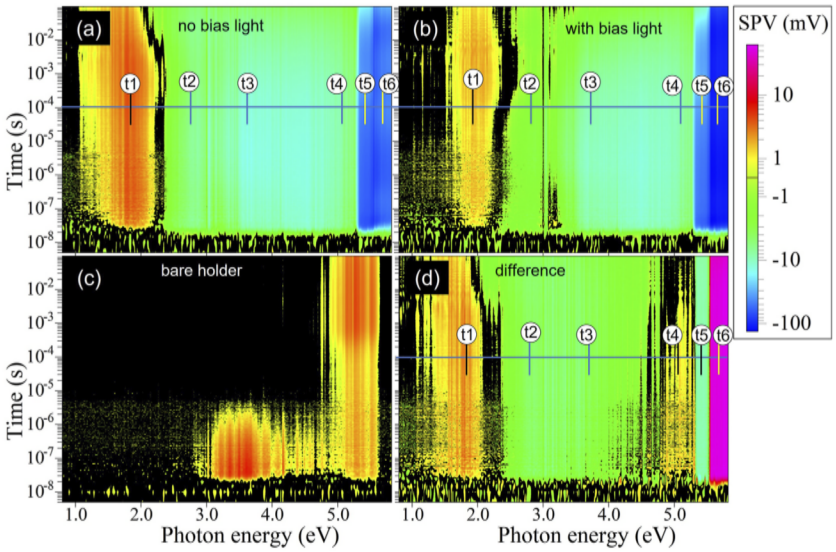

FIG. 1. Contour plots of transient SPV spectroscopy for diamond (a) without and (b) with bias light from a white LED, (c) the bare sample holder, and (d) the difference between the contour plots for diamond without and with bias light. The markers (t1–t6) along the line at 100 μs mark points at characteristic photon energies (1.82, 2.8, 3.7, 5.12, 5.39, and 5.61 eV, respectively) of the contour plots [(a), (b), and (d)]. Keep in mind the logarithmic color scale for the SPV signals.

Since the illumination conditions for parasitic signals also depend on the presence of the diamond sample, the suitable influence of parasitic SPV signals can be eliminated by analyzing the difference contour plot between measurements without and with bias light [Fig. 1(d)]. In the difference contour plot, the region with t1 remained the same, the regions with t2 and t3 merged into one region, the region with t4 showed weak positive differences and extended to lower photon energies at about 4.8 eV, and the regions with t5 and t6 remained the same. However, differences of about −10 mV (region with t5) and up to +60 mV (region with t6) were practically constant over the whole range shown, and the boundaries between regions with t4 and t5 and with t5 and t6 were relatively sharp.

Figure 2 shows SPV transients measured without and with bias light and difference transients obtained at characteristic photon energies in t1–t6 [(a) t1–t4 and (b) t5 and t6]. All transients measured without and with bias light showed a fast increase within the resolution time of the system. At longer times, pronounced local minima and maxima appeared in the transients measured without and with bias light (one shall keep in mind that minima and maxima belong to absolute values). The times at which local minima and maxima appeared (t_{min} and t_{max}, respectively) were independent of measurement without and with bias light. In the following, values of t_{min} and t_{max} are given with respect to the time at which the laser pulses were switching on. For t1, a local minimum and maximum appeared at t_{min} = 20 μs and t_{max} = 500 μs, respectively. For t2, two local minima and maxima appeared at t_{min} = 0.3 μs and 2 ms and at t_{max} = 5 μs and 20 ms, respectively. For t3 and t4, only one local maximum was observed at t_{max} = 4 and 20 μs, respectively. The transients for t5 showed a short peak of about 6 mV decaying within about 0.25 μs and a local minimum and maximum at t_{min} = 400 μs and t_{max} = 3 ms, respectively. For t6, three local minima and maxima were distinguished at t_{min} = 0.25, 90 μs and 1.8 ms and at t_{max} = 1.3, 440 μs and 15 ms, respectively.

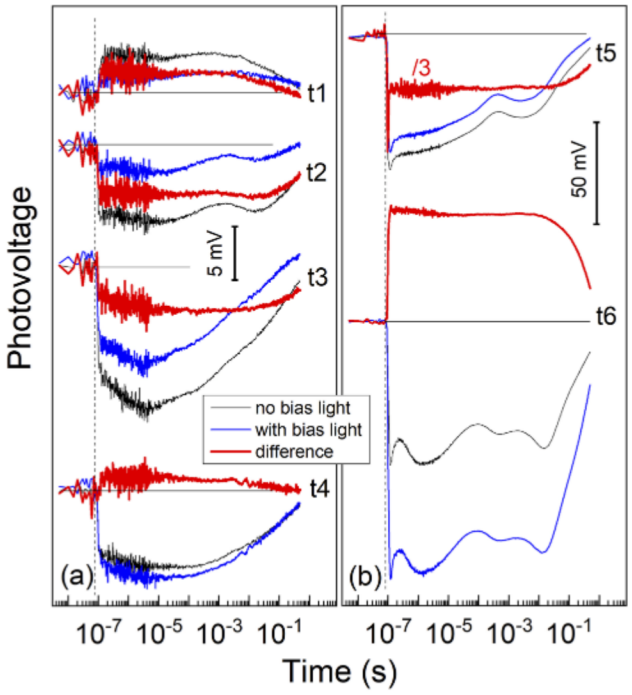

FIG. 2. SPV transients measured without and with bias light (thin black and medium blue line, respectively) and difference transients (thick red lines) obtained at characteristic photon energies t1–t6 for excitation below [(a), t1–t4] or close to and above the bandgap of diamond [(b), t5 and t6]. The thin dashed and solid lines mark the onset time of the laser pulses and the baselines of the transients, respectively.

The highest SPV signals were obtained for t6 (−70 and −127 mV for measurement without bias and with bias light, respectively) whereas the maximum SPV signals appeared within 20–25 ns. The maximum SPV signals were related to charge separation in built-in electric fields since drift times are much shorter than 20 ns in diamond, i.e., the maximum SPV signals can be assigned to values close to the surface band bending. However, one shall keep in mind that this surface band bending is not related to equilibrium since it is influenced by separated charge not relaxing within the time between two subsequent laser pulses. The increase of negative surface band bending under bias illumination with photon energies below the bandgap means that photogenerated holes were preferentially trapped at surface states.

Local minima and maxima in SPV transients are caused by the evolution of charge separation processes with different dynamic behaviors and in the opposite direction. For example, a local maximum evolved in negative SPV transients of moderately p-type doped silicon due to the overlap of electrons drifting in the built-in electric field toward the surface (negative sign) and of electrons diffusing faster than holes toward the bulk (positive sign, Dember photovoltage).[23] For diamond, one would expect a negative Dember photovoltage since the mobility of holes is higher than that of electrons. As another example, local minima and maxima appeared in SPV transients of perovskite layers depending on trapping and emission of charge carriers at charge-selective buried interfaces.[19,24] Therefore, processes in the bulk and at the surface of diamond can be responsible for the evolution of local minima and maxima in SPV transients. However, for the unambiguous identification of processes dominating in the different time domains of SPV transients, complex experiments with systematic changes in thickness, doping, surface conditioning, etc., are required.

Surprisingly, the local minima and maxima appearing in SPV transients measured without and with weak visible bias light disappeared practically completely in the difference transients (Fig. 2). Therefore, the processes leading to the evolution of local minima and maxima in SPV transients were independent of built-in electric fields. Furthermore, the decays of the larger difference transients of the dominating regions could be fitted by stretched exponentials with time constants of the order of hundreds of ms and stretching parameters between about 0.4 and 0.9 whereas the stretching parameters tended to increase with increasing amplitude. Therefore, the decay of the difference transients was limited by relaxation between two subsequent laser pulses, and the relaxation depended on the occupation of deep traps in the bulk of diamond.

Figure 3 compares the spectra of the photon flux and the transmission of the investigated diamond in the range of the indirect bandgap with the spectra of the SPV signals obtained at 20 ns and

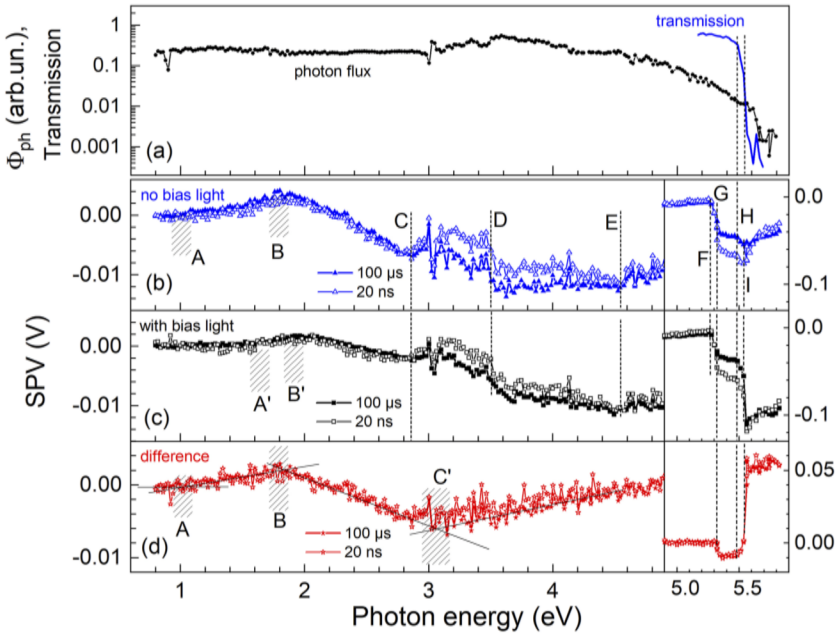

FIG. 3. Spectra of the photon flux and of the transmission of diamond in the range of the indirect bandgap [(a), black circles and blue line, respectively] and of the SPV signals obtained at 20 ns (open symbols) and 100 μs (filled symbols) after the onset of the laser pulses for measurements without and with bias light [(b) and (c), respectively] and the corresponding difference signals (d). Keep in mind the different scales for the SPV signals at the right and left sides in (b)–(c). The dashed lines and the hatched areas mark characteristic transitions designated also by the capital letters A–I. Transitions C, D, and E in (b) and (c) vanished in the difference spectra (d). As an example, the thin lines in (d) were used to determine the transitions A, B, and C′.

100 μs after the onset of the laser pulses measured without and with bias light and the corresponding difference signals.

Excitation at photon energies below the bandgap is considered first. For the spectra of the SPV signals measured without bias light, positive SPV signals were set at photon energies around 1 eV (transition A). Around 1.8 eV, the SPV signals started to become negative (transition B). At about 2.9 eV, the SPV signals started to become more positive (transition C) and more negative at 3.5 eV (transition D). The SPV signals started to slightly become more positive at about 4.5 eV (transition E). For the spectra of the SPV signals measured with bias light, the onsets of transitions A and B shifted to 1.3 and 1.9 eV (transitions A′ and B′, respectively), whereas the onsets of transitions C–E remained the same. For the difference spectra, transitions C–E disappeared, i.e., these transitions were caused by the sample holder. Furthermore, a new transition C′ appeared at about 3.1 eV. This transition was masked in the previous spectra by transitions C and D. The continuous change in the difference signals above 3.1 eV toward a positive sign gives evidence that the change in the sign around 4.8 eV [see Fig. 1(d)] was not a signature of an additional transition. Therefore, defect transitions leading to more negative or positive charging at the diamond surface were distinguished at about 1 and 3.1 eV and at about 1.8 eV (A and C′, and B, respectively). These transitions are in the same range of photon energies as transitions observed by photocurrent measurements on undoped (1.0 and 3.0 eV) and N (1.7 eV) doped diamond.[25] On the other hand, no signatures were observed by transient SPV spectroscopy for transitions at 2.3 and 4.2 eV (photocurrent measurements on undoped diamond[25]).

In the region near the bandgap of diamond, several transitions could be distinguished. At a photon energy of 5.27 eV (transition F), the SPV signals changed identically to negative values for measurements at 20 ns and 100 μs for the measurements without and with bias light. Transition F disappeared in the difference spectrum. This means that excitation at transition F resulted in transport processes independent of bias light, i.e., separation in space and relaxation of charge carriers excited via transition F was independent of the built-in electric field.

The slope of the change to higher negative SPV signals decreased strongly at about 5.32 eV (transition G) for the measurements without and with bias light whereas the change to higher negative SPV signals was stronger for the measurement at 20 ns. The difference signals became negative at transition G, i.e., the negative SPV signals decreased for the measurement without bias light. Separation of charge carriers excited via transition G showed, therefore, a decrease in the built-in electric field under bias illumination, i.e., a reduction of holes trapped at surface states.

At 5.48 eV (transition H), the slope of the change to higher negative SPV signals increased for the measurements without and with bias light. The negative difference signals between the measurements with and without bias light started to decrease at transition H.

The strongest and qualitatively different changes were observed at photon energies larger than 5.53 eV (transition I). At transition I, the SPV signals measured without bias light started to change to lower negative signals. In contrast, the SPV signals measured with bias light showed a sharp increase at transition I. The onset of transition I was accompanied by a change in the sign of the difference signals and a steep increase from 2 to 40 and 58 mV at 5.53 and 5.56 eV, respectively. On observation, the transmission of the investigated diamond decreased by about 30 times (up to the noise level) between 5.53 and 5.56 eV whereas the photon flux remained practically constant in this small interval, i.e., the density of photogenerated charge carriers increased drastically. At photon energies above 5.56 eV, the negative SPV signals measured

with bias light decreased due to the strong decrease in the photon flux. The difference signals between the measurements with and without bias light remained practically constant at higher photon energies of above 5.56 eV. Separation of charge carriers excited via transition I showed a strong increase in the built-in electric field under bias illumination, i.e., an increase in holes trapped at surface states.

Diamond has an indirect bandgap at E_g = 5.470 ± 0.005 eV whereas optical absorption is accompanied by an indirect exciton with a binding energy of E_x = 0.070 ± 0.004 eV.[1] An absorption event near an indirect bandgap is assisted by emission or absorption of a phonon. In diamond, the energies of the transverse optical, the longitudinal optical and acoustical, and the transverse acoustical phonons are $h\nu_{TO}$ = 0.143 ± 0.002 eV, $h\nu_{LO,LA}$ = 0.132 ± 0.002 eV, and $h\nu_{TA}$ = 0.083 ± 0.003 eV, respectively.[1] Figure 4 gives a closer view of the SPV spectra obtained at 20 ns in the region near the bandgap together with energies E_g–E_x, E_g–E_x ± $h\nu_{TO}$, E_g–E_x ± $h\nu_{LO,LA}$, and E_g–E_x ± $h\nu_{TA}$.

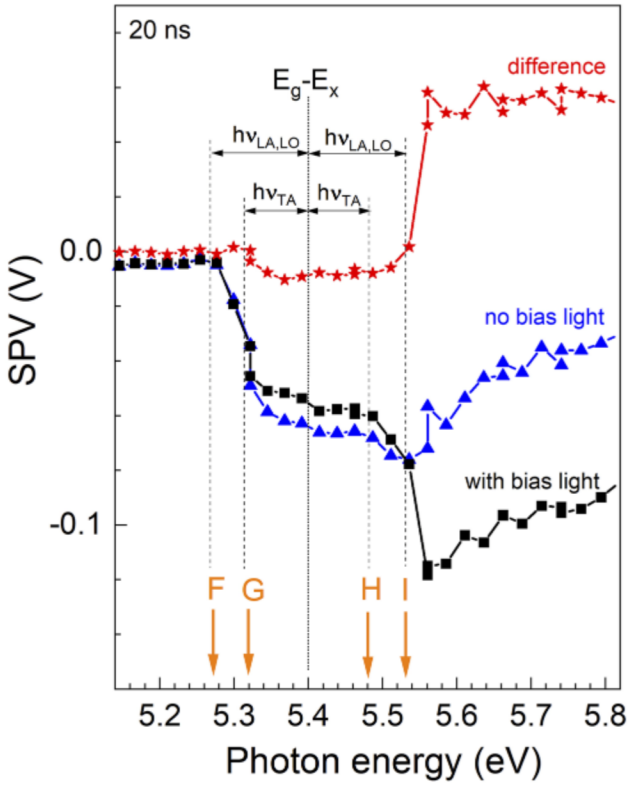

FIG. 4. Spectra of the SPV signals obtained at 20 ns (data also shown in Fig. 3) after the onset of the laser pulses for measurements without and with bias light (blue triangles and black squares, respectively) and the corresponding difference signals (red stars). The dotted line marks the difference between the indirect bandgap and the binding energy of the indirect exciton of diamond (E_g–E_x). The thin dashed lines mark the differences and sums between E_g–E_x and phonon energies (shown by arrows and marked by $h\nu$, whereas the indices TA, LA, and LO denote transverse acoustical, longitudinal acoustical, and longitudinal optical phonons, respectively). The orange arrows and the capital letters F–I mark the measured characteristic transitions, also shown in Fig. 3.

Within the experimental errors, transitions G (5.32 eV) and H (5.48 eV) could be well assigned to E_g–E_x ± $h\nu_{TA}$, respectively. Transitions F (5.27 eV) and I (5.53 eV) were closer to E_g–E_x ± $h\nu_{LO,LA}$ than to E_g–E_x ± $h\nu_{TO}$, respectively. In this context, transitions F, G, H, and I correspond to the absorption components denoted as E_3 (5.268 eV), E_4 (5.314 eV), E_7 (5.482 eV), and E_9 (5.531 eV), respectively, in Ref. 1.

The relatively weak visible bias light had a very different influence on the behavior of SPV signals related to transitions E_g–E_x-$h\nu_{LO,LA}$ (no influence) and E_g–E_x + $h\nu_{LO,LA}$ (reduction vs strong increase in negative signals for measurement without and with bias light, respectively). The transport of excitons is not affected by electric fields, and excitons do not contribute to SPV signals. It seems that SPV signals induced by absorption at E_x-$h\nu_{LO,LA}$ were related to dissociation of excitons at localized states at/near the surface and subsequent directed charge transfer. On the other hand, absorption above E_x + $h\nu_{LO,LA}$ caused excitation of free charge carriers being separated within the built-in electric field.

IV. CONCLUSIONS

It has been shown for the first time that transient SPV spectroscopy with a charge amplifier has great potential for contactless and highly sensitive characterization of electronic transitions below and around the bandgap of diamond.

The application of weak visible bias light allowed for the elimination of a possible impact of SPV signals not related to diamond and originating, for example, from charge separation in/at other illuminated materials used in the sample holder, electrode, and connecting wire. The application of weak visible bias light was especially important for the unambiguous detection of weak SPV signals caused by excitation from defect states below the bandgap of diamond. Transitions related to defect states in diamond were found at about 1.0, 1.8, and 3.1 eV.

In addition, the application of weak visible bias light allowed distinction between charge separation processes depending and not depending on a built-in electric field. Weak bias light led to increased trapping of positive charge at the diamond surface so that the negative band bending increased. This gave additional information about transport processes for excitation near the bandgap of diamond where absorption is assisted by an indirect exciton and by phonons.

Transitions near the bandgap of diamond were observed by transient SPV spectroscopy at 5.27, 5.32, 5.48, and 5.53 eV and could be assigned to absorption assisted by an indirect exciton and absorption of longitudinal optical and acoustic, absorption of transverse acoustic, emission of transverse acoustic, and emission of longitudinal optical and acoustic phonons, respectively.

It has been demonstrated that transport related to exciton diffusion followed by exciton dissociation and directed charge transfer (example: transition at 5.27 eV) can be distinguished from separation of mobile charge carriers in built-in electric fields (example: transition at 5.53 eV). The appearance of pronounced local minima and maxima in SPV transients measured without and with bias light and their disappearance in difference transients give further evidence to exciton diffusion, dissociation of excitons, and specific charge transfer. However, the effect of charge separation by exciton dissociation in diamond shall be verified and studied in more detail

for a larger amount of diamond crystals prepared under different conditions.

In the future, it will be important to more precisely distinguish between defect states in the bulk and at the surface of diamond as well as their impact on processes of charge separation and relaxation. For this purpose, the approach of transient SPV spectroscopy with a charge amplifier will be extended to experiments under well controlled conditions in ultra-high vacuum over wide temperature ranges.

ACKNOWLEDGMENTS

The author acknowledges Freiberg Instruments for providing the diamond crystal and the AiF (project Grant No. ZIM-KK 5085302DF0) for financial support and thanks S. Fengler and I. Levine for discussions.

AUTHOR DECLARATIONS

Conflict of Interest

The author has no conflicts of interest to disclose.

DATA AVAILABILITY

The data that support the findings of this study are available from the author upon reasonable request.

REFERENCES

[1]C. D. Clark, P. J. Dean, and P. V. Harris, Proc. R. Soc. London, Ser. A **277**, 312 (1964).
[2]J. Pernot, C. Tavares, E. Gheeraert, E. Bustarret, M. Katagiri, and S. Koizumi, Appl. Phys. Lett. **89**, 122111 (2006).
[3]J. Pernot, P. N. Volpe, F. Omnès, P. Muret, V. Mortet, K. Haenen, and T. Teraji, Phys. Rev. B **81**, 205203 (2010).
[4]H. Umezawa, Mater. Sci. Semicond. Process. **78**, 147 (2018).
[5]P. Liu, R. Yen, and N. Bloembergen, IEEE J. Quantum Electron. **14**, 574 (1978).
[6]G. A. Slack, J. Appl. Phys. **35**, 3460 (1964).
[7]C. Schreyvogel, V. Polyakov, R. Wunderlich, J. Meijer, and C. E. Nebel, Sci. Rep. **5**, 12160 (2015).
[8]E. Bourgeois, A. Jarmola, P. Siyushev, M. Gulka, J. Hruby, F. Jelezko, D. Budker, and M. Nesladek, Nat. Commun. **6**, 8577 (2015).
[9]H.-C. Lu, J.-I. Lo, Y.-C. Peng, S.-L. Chou, B.-M. Cheng, and H.-C. Chang, ACS Appl. Mater. Interfaces **12**, 3847 (2020).
[10]See, for example, the review: J. Raymakers, K. Haenen, and W. Maes, J. Mater. Chem. C **7**, 10134 (2019).
[11]See, for example, the review: K. G. Crawford, I. Maini, D. A. MacDonald, and D. A. J. Moran, Prog. Surf. Sci. **96**, 100613 (2021).
[12]L. Kronik and Y. Shapira, Surf. Sci. Rep. **37**, 1 (1999).
[13]T. Dittrich and S. Fengler, *Surface Photovoltage Analysis of Photoactive Materials* (World Scientific Publishing Europe, Ltd., London, 2020).
[14]B. Rezek and C. E. Nebel, Diamond Relat. Mater. **14**, 466 (2005).
[15]A. Hoffman, A. Lafosse, R. Akhvlediani, and R. Azria, Diamond Relat. Mater. **16**, 851((2007).
[16]S. Challinger, I. Baikie, and A. G. Birdwell, MRS Adv. **2**, 2229 2017).
[17]G. T. Williams, S. P. Cooil, O. R. Roberts, S. Evans, D. P. Langstaff, and D. A. Evans, Appl. Phys. Lett. **105**, 061602 (2014).
[18]S. Challinger, I. Baikie, A. G. Birdwell, and S. Strehle, Phys. Status Solidi C **14**, 1700152 (2017).
[19]I. Levine, A. Al-Ashouri, A. Musijenko, H. Hempel, A. Magomedov, A. Drevilkauskaite, V. Getautis, D. Menzel, K. Hinrichs, T. Unold, S. Albrecht, and T. Dittrich, Joule **5**, 2915 (2021).
[20]T. Dittrich, L. E. Valle Rios, S. Kapil, G. Gurieva, N. Rujisamphan, and S. Schorr, Appl. Phys. Lett. **110**, 023901 (2017).
[21]S. Fengler, H. Kriegel, M. Schieda, H. Gutzmann, T. Klassen, M. Wollgarten, and T. Dittrich, ACS Appl. Mater. Interfaces **12**, 3140 (2020).
[22]T. Dittrich, S. Fengler, and N. Nickel, Phys. Status Solidi A **218**, 2100167 (2021).
[23]K. Heilig, Surf. Sci. **44**, 421 (1974).
[24]T. S. Ntia, T. Supasai, I. M. Tang, V. Amornkitbumrung, J. Yuan, Y. Li, T. Dittrich, and N. Rujisamphan, Phys. Status Solidi A **216**, 1900087 (2019).
[25]E. Rohrer, C. E. Nebel, M. Stutzmann, A. Flöter, R. Zachai, X. Jiang, and C.-P. Klages, Diamond Relat. Mater. **7**, 879 (1998).